Physics Letters A 380 (2016) 3625–3629

Contents lists available at ScienceDirect

Physics Letters A

www.elsevier.com/locate/pla

Maximal intensity higher-order Akhmediev breathers of the nonlinear Schrödinger equation and their systematic generation

Siu A. Chin [a,*], Omar A. Ashour [a,b], Stanko N. Nikolić [b,c], Milivoj R. Belić [b]

[a] Department of Physics and Astronomy, Texas A&M University, College Station, TX 77843, USA
[b] Science Program, Texas A&M University at Qatar, P.O. Box 23874 Doha, Qatar
[c] Institute of Physics, University of Belgrade, Pregrevica 118, 11080 Belgrade, Serbia

ARTICLE INFO

Article history:
Received 13 July 2016
Received in revised form 16 August 2016
Accepted 17 August 2016
Available online 27 August 2016
Communicated by C.R. Doering

Keywords:
Nonlinear Schrödinger equation
Akhedmiev breathers
Darboux transformation
Optical solitons
Rogue waves
High intensity light pulse

ABSTRACT

It is well known that Akhmediev breathers of the nonlinear cubic Schrödinger equation can be superposed nonlinearly via the Darboux transformation to yield breathers of higher order. Surprisingly, we find that the peak height of each Akhmediev breather only adds *linearly* to form the peak height of the final breather. Using this peak-height formula, we show that at any given periodicity, there exists a unique high-order breather of maximal intensity. Moreover, these high-order breathers form a continuous hierarchy, growing in intensity with increasing periodicity. For any such higher-order breather, a simple initial wave function can be extracted from the Darboux transformation to dynamically generate that breather from the nonlinear Schrödinger equation.

The study of high-intensity optical solitons on a finite background, known as "breathers" (and "rogue waves"), is of growing importance in modern nonlinear photonics. For a comprehensive reference of recent works, see the review by Dudley et al. [1]. One way of achieving high intensity is to create higher-order versions of these breathers. (We regard rogue waves as special cases of breathers with infinite period [2].) While it has been known for a long time [3] that these higher-order breathers can be composed from first-order breathers via the Darboux transformation (DT), the recursive complexity of the transformation [3–7] has obscured insights into the working of DT's nonlinear superposition. In this work, we find analytically that, despite the nonlinear superposition, the peak heights of the breathers only add *linearly*. From this key result, one can prove that: I) At each periodicity, there is a unique higher order breather of *maximal* peak intensity. II) With increasing periodicity, these higher-order breathers form a continuous hierarchy of single-peak solitary waves with monotonically rising intensity. III) In the limit of an infinite period, these higher-order breathers morph smoothly into rational rogue waves of the same order. IV) From the breather's numerical wave function produced by DT, an initial wave function in the form of a cosine series can be extracted, so that when the latter is inputted into the nonlinear Schrödinger equation (NLSE), the breather can be generated *dynamically*. Since the NLSE is an excellent model for propagating light pulses in an optical fiber, our results strongly suggest that breathers of extreme intensity and short duration can be systematically produced in optical fibers.

Let's first summarize some well-known properties of first-order Akhmediev breathers (ABs) [8,9]. The breather's wave function

$$\psi(t,x)=\left[1+\frac{2(1-2a)\cosh(\lambda t)+i\lambda\sinh(\lambda t)}{\sqrt{2a}\cos(\Omega x)-\cosh(\lambda t)}\right]e^{it}, \tag{1}$$

is an exact solution to the cubic NLSE

$$i\frac{\partial\psi}{\partial t}+\frac{1}{2}\frac{\partial^2\psi}{\partial x^2}+|\psi|^2\psi=0, \tag{2}$$

on a finite background: $|\psi(t\to\pm\infty,x)|\to 1$. Its most fundamental characteristic is that it is *periodic* over a length L parametrized by the modulation parameter a:

$$L=\pi/\sqrt{1-2a}.$$

Only in the singular limit of $a\to 1/2$, $L\to\infty$, does it become the non-periodic, Peregrine soliton [10].

At a given a, because of this basic periodicity, the allowed Fourier modes can only have wave numbers

$$k_m=m\Omega \qquad \text{for} \quad m=0,\pm1,\pm2,\cdots, \tag{3}$$

* Corresponding author.
E-mail address: chin@physics.tamu.edu (S.A. Chin).

http://dx.doi.org/10.1016/j.physleta.2016.08.038
0375-9601/

where Ω is the interval's fundamental wave number:

$$\Omega = 2\pi/L = 2\sqrt{1-2a}. \tag{4}$$

The growth factor $\lambda = \sqrt{8a(1-2a)} = \Omega\sqrt{1-(\Omega/2)^2}$ is due to the instability of this fundamental mode, as determined by the Bogoliubov spectrum [11–13] or by the Benjamin–Feir [14] instability. This growth factor, when real, implies that all modes with $|k_m| < 2$ are unstable. Specifically, the first nonzero $|m|$ harmonic modes are unstable for $|m|\Omega < 2$, or at the parameter values [15]

$$a > a_m^* \equiv \frac{1}{2}\left(1 - \frac{1}{m^2}\right). \tag{5}$$

If a *were* negative, then (4) implies that $\Omega > 2$ and all modes are stable. A negative a will therefore not result in an AB, but only in stable Bogoliubov excitation modes [13].

The AB wave function (1) peaks at $t = 0$, with profile

$$\psi(0,x) = 1 + \frac{2(1-2a)}{\sqrt{2a}\cos(\Omega x) - 1}. \tag{6}$$

The maximum peak height is at $x = 0$,

$$|\psi|_{max} = 1 + 2\sqrt{2a}. \tag{7}$$

As a increases from 0 to 1/2, this peak height increases from the background height of 1 and smoothly matches the Peregrine's [10] peak height of 3.

By using DT, an nth-order breather can be constructed from n ABs with an arbitrary set of real modulation parameters

$$a_1 > a_2 > a_3 > \cdots a_n > 0. \tag{8}$$

(All t- and x-shift parameters [6] are set to zero.) However, such a construction would overlook the importance of periodicity. Given an initial AB with $a_1 = a$, it is periodic over a length of $L_1 = L$. For any $a_k < a_1$, the resulting Ω_k, if incommensurate with Ω, would completely destroy the periodicity of the original AB. Even if Ω_k were commensurate with Ω, unless Ω_k is just a multiple of Ω, the periodic length L must be enlarged to accommodate both wave numbers. While there is no logical argument forbidding such an arbitrary a_k construction, it is reasonable to insist that the higher-order breather retains the same periodic length L as the initial AB. In this case, one must choose $\Omega_k = k\Omega$, resulting in the following set of modulation parameters:

$$a_k = k^2\left(a - \frac{1}{2}\right) + \frac{1}{2}. \tag{9}$$

This set of a_k as a function of a is plotted in Fig. 1. Note that $a_k > 0$ only when $a > a_k^*$. Let's denote the region $a_n^* < a < a_{n+1}^*$ as R_n; then in each region R_n there are exactly n values of (8) that can be combined by DT to form an nth-order breather. We will show below that such a breather has the highest peak intensity at any given periodic length parametrized by a.

The Darboux transformation gives

$$\psi_n(t,x) = \psi_{n-1}(t,x) + \delta\psi(t,x), \tag{10}$$

where $\delta\psi(t,x)$ depends *recursively* on all the previous-order wave functions [3–6]. This is classic nonlinear superposition. However, we will prove in the Appendix that for an nth-order AB, the maximum peak height at $t=0$ and $x=0$ only adds *linearly*, given by

$$|\psi|_{max} = 1 + 2\sum_{k=1}^{n}\sqrt{2a_k}. \tag{11}$$

This is one key finding of this work, valid for an arbitrary set of real a_k.

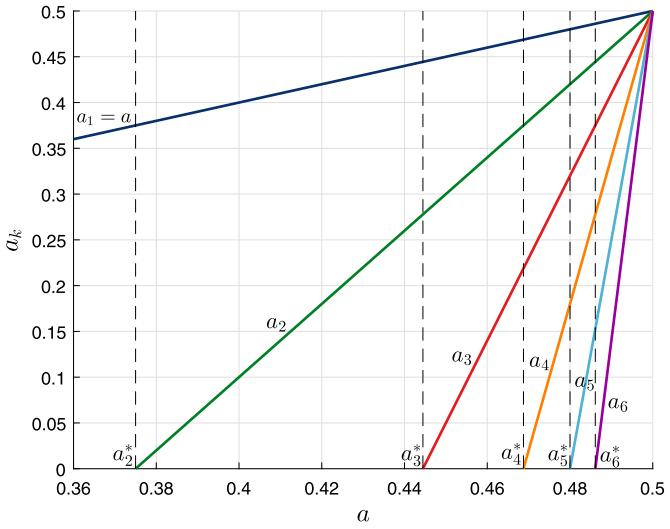

Fig. 1. Modulation parameters a_k of (9) as functions of a. Vertical broken lines indicate the locations of a_m^*.

The peak height of $|\psi(0,0)|$ has been studied previously. In an early work of Akhmediev and Mitzkevich [16], a formula similar to (11) was stated without proof for solitons, in terms of the imaginary parts of DT eigenvalues. (For an AB, the corresponding imaginary part is $\sqrt{2a}$.) More recently, Kedziora, Ankiewicz and Akhmediev [17] have found *numerically* that the peak amplitude of a fused n-order rogue wave is one plus twice the imaginary part times n, corresponding to (11) with all a_k equal. Later in Ref. [18], a case (their Fig. 8) with three different imaginary parts is also found to be true, numerically. However, in all these cases, the term with the imaginary part was never explicitly identified as the peak-height of the constituent breather or soliton.

For the special set of a_k given by (9), we can further deduce that: 1) In each region of R_n there is a unique nth-order AB with peak height given by (11). This peak height is maximal because it is a sum over all available and possible a_k's of a given periodic length. 2) In regions lower than R_n, this nth-order AB does not exist because some of the required a_k are not positive. 3) In regions higher than R_n, this nth-order AB retains the highest peak height among all nth-order ABs. For example, in R_3, we have $a_1 > a_2 > a_3 > 0$. Clearly, from Fig. 1 and (11), the second-order AB formed from a_1 and a_2 will have the greater peak height than the AB2 formed from a_1 and a_3 or a_2 and a_3. The last case also illustrates that the peak height of an AB2 formed from any two a values having commensurate wave numbers will always be lower than that formed from wave numbers k_1 and k_2 over the *same* periodic interval. Therefore, by (11), the nth-order AB formed from the first n values of (9) has peak intensity greater than any other AB having the same periodic length.

The peak heights of these maximal higher-order ABs are plotted in Fig. 2. In each R_n region, the maximal intensity breather is indicated as a solid line. These solid lines can be joined continuously over each region, forming a single hierarchy of maximal intensity breathers. In higher R_n regions, the lower-order ABs remain maximal for their order and are denoted by broken lines. As $a \to 1/2$, (11) smoothly yields $|\psi|_{max} = 1 + 2n$, which are the peak heights of nth-order *rational* rogue waves (RWs) [2]. Thus, RWs are the natural end points of our periodic ABs. Although RWs have the highest intensity at each order, their intensities are discrete, with ever-growing gaps between successive orders. By contrast, the intensity of our hierarchy of periodic ABn, as shown in Fig. 2, can be continuously chosen by changing the periodic length via the modulation parameter a.

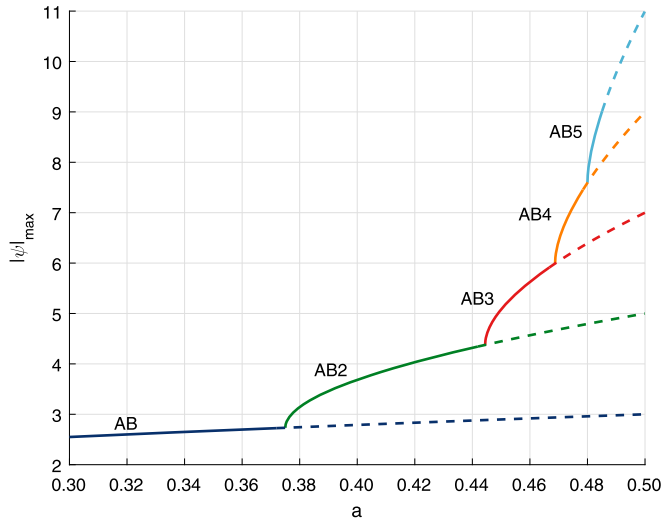

Fig. 2. Peak heights of maximal intensity nth-order Akhmediev breathers at any spatial periodic length parametrized by the modulation parameter a.

Now that we have shown that this hierarchy of high-order ABs is of maximal intensity, the next step is to find ways of producing them *systematically*. Currently, only breathers up to the second-order have been observed in optical fibers [19–21]. While third-order breathers have been seen in random field searches [1,22], the analytical initial wave functions used for exciting a second-order RW optically [20], or a third-order RW theoretically [23], were essentially obtained by trial and error.

Recall that the AB wave function at $t=0$, (6), is an *even* function of x. Since the NLSE preserves the symmetry of the wave function, the full wave function must remain spatially symmetric [8], in the form of

$$\psi(t,x) = A_0(t) + 2\sum_{m=1}^{\infty} A_m(t)\cos(m\Omega x), \tag{12}$$

with complex amplitudes $A_m(t)$. As shown in Ref. [24], the instability of the fundamental mode $A_1(t)$ induces a cascading instability of all the $|m|>1$ modes, causing all to grow exponentially in locked-step with $A_1(t)$, as $|A_m(t)|\sim|A_1(t)|^{|m|}$. Therefore, at a long time *before* the AB peak, all higher-mode amplitudes are exponentially small, as compared to $A_1(t)$, and the wave function must be of the form

$$\psi_0(x) = A_0 + 2A_1\cos(\Omega x), \tag{13}$$

with complex amplitudes $A_0\sim 1$ and $A_1\sim 0$. Similarly, for an nth-order AB, with n unstable modes, the wave function at a long time before the peak must be of the form

$$\psi_0(x) = A_0 + 2\sum_{m=1}^{n} A_m\cos(m\Omega x), \tag{14}$$

with n complex coefficients A_m shaping the growth of the n unstable modes into a single nth-order AB. Clearly, any trial and error, or grid-search method would be impractical for determining more than two A_m coefficients.

Here, we propose an extremely simple, yet systematic way of determining these coefficients. The method is to use the Darboux transformation to generate a numerical nth-order AB wave function at a sufficiently long time before the peak and extract the n coefficients A_m by *fitting* it with the functional form (14). (The constant A_0 is fixed by normalization.)

Figs. 3 and 4 show the resulting second-order AB at $a=0.43$, produced from the NLSE with the $n=2$ initial wave function (14).

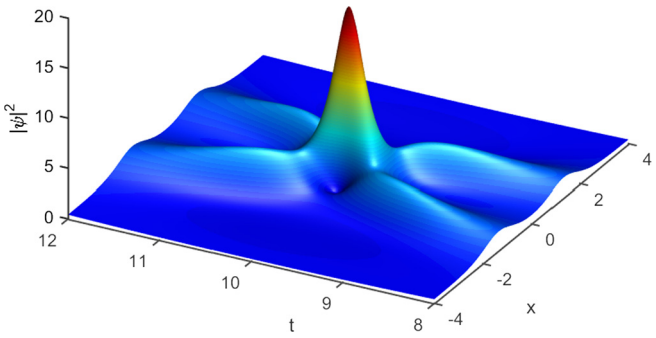

Fig. 3. (Color online.) Second-order Akhmediev breather at $a=0.43$, generated from the nonlinear Schrödinger equation using initial wave function (14). Coefficients are fitted from the Darboux transformation at $t=10$ before the peak; $A_1=(0.532+1.32i)10^{-3}$, $A_2=(-7.56-6.54i)10^{-5}$, $|\psi|^2_{max}=17.48$ (17.48). The value in parentheses gives the maximum intensity according to Eq. (11).

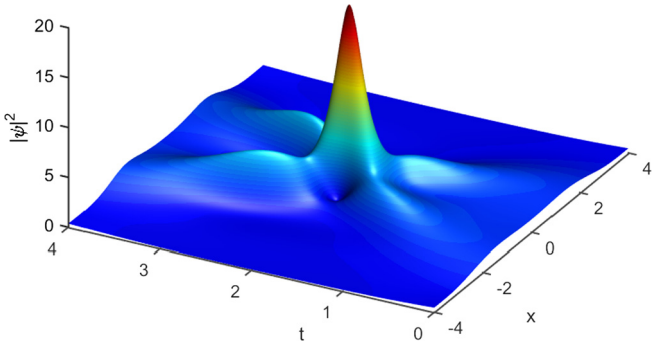

Fig. 4. (Color online.) Same as Fig. 3, but with coefficients fitted at $t=2$ before the peak, with only two decimal places, $A_1=0.18+0.28i$, $A_2=-0.11-0.03i$, $|\psi|^2_{max}=18.61$ (17.48). This second-order AB is asymmetric.

The NLSE was solved numerically using a second-order splitting fast Fourier transform method with time step $\Delta t=0.0001$ and double-checked using a fourth-order symplectic splitting scheme [25]. We extracted the coefficients by fitting (14) to the DT wave function at $t=-2$ and at $t=-10$. (Therefore, when solving the NLSE numerically, the peak appears at $t=2$ and $t=10$ simulation time.) Since an overall phase is irrelevant, we subtract the phase of A_0 from all coefficients, so that A_0 is real and we renormalize it, to obtain $A_0=\sqrt{1-2|A_1|^2-2|A_2|^2}$. Thus, only two complex numbers for A_1 and A_2 suffice.

The fitted coefficients from $t=-10$ generate a nearly-perfect reproduction of the AB2 generated from DT, with symmetric two-lobes before and after the peak. The spectral "fingerprint" shown in Fig. 5 is indistinguishable from the exact DT spectrum. The fit at $t=-2$ yields larger coefficients and produces a rather distorted/asymmetric two-lobe structure in Fig. 4 and an asymmetric spectral fingerprint in Fig. 6. Yet, despite such a distortion, the latter AB2 has slightly higher peak intensity than predicted by (11).

The use of DT to analyze numerical simulations and experiments has been done by Erkintalo et al. [15] at the same value of $a=0.43$ (see their Fig. 1). However, they used the t-shift parameter in DT to displace the two AB, so that they only get a 1-2 peak structure, rather than an AB2. One *cannot* reproduce an AB2, unless one uses the initial wave function of the form (14).

In Fig. 7 we show the resulting AB3 at $a=0.464$, a value used in the experiment of Ref. [15]. It is a relatively poor approximation to an exact AB3, similar to Fig. 4. In Figs. 8 and 9, we show intensities of AB4 and AB5, obtained in a much better approximation. For these two breathers, one must fit (14) at $t=-8$ and $t=-13$ respectively, yielding rather small but accurate coefficients.

Since an nth-order AB is composed of n ABs with wave numbers Ω, 2Ω, $\cdots$ $n\Omega$, each having 1, 2, 3, $\cdots$ n peaks respectively,

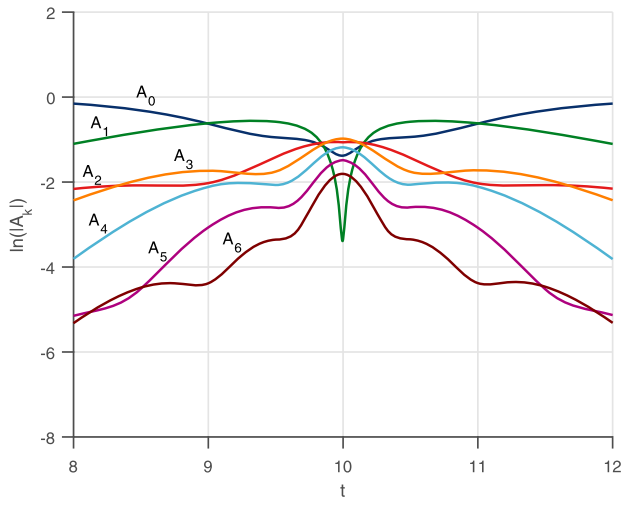

Fig. 5. (Color online.) The spectral "fingerprint" of Fig. 3, with coefficients fitted at $t=10$ before the peak. The amplitudes are perfectly symmetric before and after the peak.

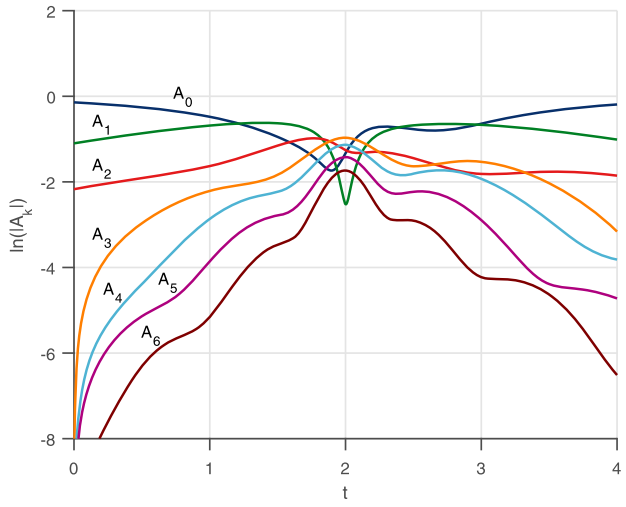

Fig. 6. (Color online.) The spectral "fingerprint" of Fig. 4, with coefficients fitted at $t=2$ before the peak. This is a poor, asymmetric imitation of Fig. 5, but the resulting AB still has comparable (actually, slightly higher) peak intensity.

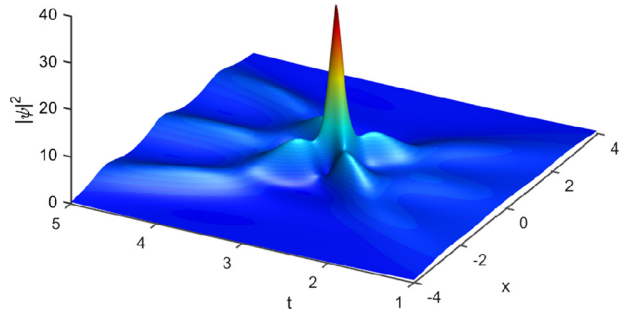

Fig. 7. (Color online.) Third-order AB at $a=0.464$ from the initial wave function (14). Coefficients are fitted at $t=3$ before the peak: $A_1=0.17+0.32i$, $A_2=-0.14+0.004i$, $A_3=0.04+0.001i$, $|\psi|^2_{max}=35.21$ (33.65). The pre-peak 3 lobes are much reduced.

it is equivalent to $1+2+\cdots n=n(n+1)/2$ single-peak ABs. This is also the observation of Ref. [5,6] on rogue waves. This composition can be seen in the evolving intensity of all nth-order ABs in each region R_n, not just in rational RWs [6]. The nth-order AB will emerge from the background with n lobes, then $(n-1)$ lobes, $(n-2)$ lobes, etc., until the intensity converges into a narrow single peak. It then decays in a time-symmetric manner back into 2 lobes, 3 lobes, $\cdots$ n lobes, and fades back into the background. In Fig. 9, we only plot the intensity near the base of the AB, to better show the evolving lobe structure described above.

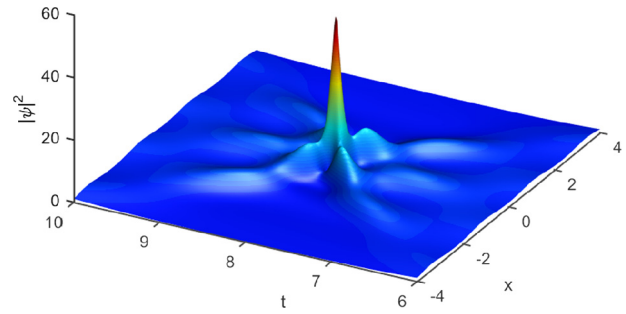

Fig. 8. (Color online.) Fourth-order AB at $a=0.47395$ from the initial wave function (14). Coefficients are fitted at $t=8$ before the peak; $A_1=0.016563+0.067661i$, $A_2=-0.005927-0.005156i$, $A_3=0.002951+0.001122i$, $A_4=-0.008055-0.003309i$, $|\psi|^2_{max}=48.57$ (49). Outer 4 lobes are at $t<6$.

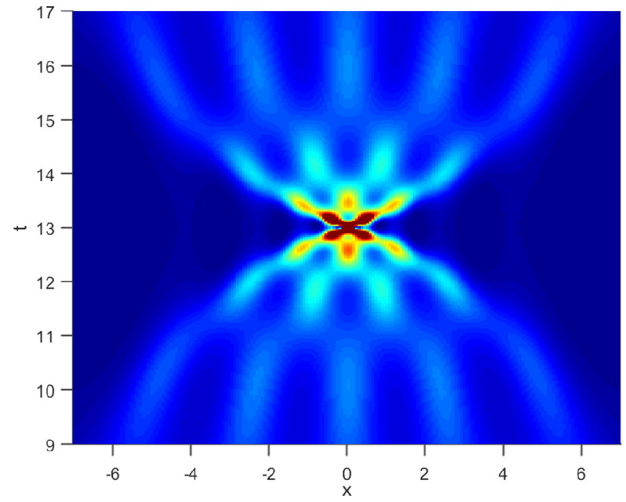

Fig. 9. (Color online.) Fifth-order AB at $a=0.4850173$ from initial wave function (14). Coefficients are fitted at $t=13$ before the peak; $A_1=(0.64382+3.6195i)10^{-2}$, $A_2=(-1.2676-1.3896i)10^{-3}$, $A_3=(1.7862+1.5434i)10^{-4}$, $A_4=(-6.6953-4.4011i)10^{-5}$, $A_5=(1.2706+0.6913i)10^{-4}$. Peak intensity is $|\psi|^2_{max}=80$ (81), but only the base with $|\psi|^2<10$ is plotted to show the time-symmetric 5-4-3-2-1-lobe structure.

Since the NLSE can model well the propagation of light pulses in an optical fiber, the above dynamical generation of high order ABs strongly suggests that they can also be produced in experiments similar to those described in Refs. [15,21]. The latter's frequency-comb can basically produce all the initial wave functions given above.

Acknowledgements

This research is supported by the Qatar National Research Fund (NPRPs 5-674-1-114 and 6-021-1-005), a member of the Qatar Foundation. S.N.N. acknowledges support from the Serbian MESTD Grants III45016 and OI171038. M.R.B. acknowledges support by the Al-Sraiya Holding Group.

Appendix. Proof of (11)

We follow the Darboux iteration in the Appendix of Ref. [6], with zero x- and t-shift parameters. The wave function at $x=0$ and $t=0$ can be evaluated starting from their Eq. (A4),

$$r_{1j}=2i\sin(A_{jr}),\quad s_{1j}=2\cos(B_{jr}),$$

$$A_{jr} = \frac{1}{2}\arccos(\frac{\Omega_j}{2}) - \frac{\pi}{4}, \quad B_{jr} = -\frac{1}{2}\arccos(\frac{\Omega_j}{2}) - \frac{\pi}{4},$$

with $\Omega_j = 2\sqrt{1-2a_j^2}$. Therefore,

$$s_{1j} = 2\cos(B_{jr}) = 2\cos(A_{jr} + \frac{\pi}{2}) = -2\sin(A_{jr}) = ir_{1j}. \tag{15}$$

Equation (15) is the only result we needed to prove our formula. It follows that for all $j \geq 1$

$$|s_{1j}|^2 = |r_{1j}|^2. \tag{16}$$

From Ref. [6]'s Eq. (A6),

$$\begin{aligned} |\psi|_{max} &= 1 + \frac{2(l_1^* - l_1)s_{11}r_{11}^*}{|r_{11}|^2 + |s_{11}|^2} = 1 + \frac{2(l_1^* - l_1)i|r_{11}|^2}{|r_{11}|^2 + |s_{11}|^2} \\ &= 1 + (l_1^* - l_1)i = 1 + (-i\sqrt{2a_1} - i\sqrt{2a_1})i \\ &= 1 + 2\sqrt{2a_1}, \end{aligned} \tag{17}$$

where $l_n = i\sqrt{2a_n}$. Note that we only need to know (15) and (16) to arrive at (17); we do not need to know the *explicit* forms of s_{11} and r_{11}.

We now prove by induction that (15) generalizes to all $n \geq 1$, for $j \geq 1$:

$$s_{nj} = ir_{nj}. \tag{18}$$

Assuming that $s_{n-1,k} = ir_{n-1,k}$ for all k, specifically $k = 1$, then Ref. [6]'s Eq. (A7) gives,

$$\begin{aligned} r_{nj} &= -\sqrt{2a_{n-1}}\, s_{n-1,j+1} + i\sqrt{2a_{j+n-1}}\, r_{n-1,j+1}, \\ s_{nj} &= \sqrt{2a_{n-1}}\, r_{n-1,j+1} + i\sqrt{2a_{j+n-1}}\, s_{n-1,j+1}. \end{aligned}$$

Now invoking $s_{n-1,k} = ir_{n-1,k}$ for $k = j+1$ then gives

$$\begin{aligned} ir_{nj} &= -i\sqrt{2a_{n-1}}\, s_{n-1,j+1} - \sqrt{2a_{j+n-1}}\, r_{n-1,j+1} \\ &= \sqrt{2a_{n-1}}\, r_{n-1,j+1} + i\sqrt{2a_{j+n-1}}\, s_{n-1,j+1} \\ &= s_{nj}. \end{aligned} \tag{19}$$

From Ref. [6]'s Eq. (A8), each a_n will only contribute a factor $2\sqrt{2a_n}$ to the maximum peak height by applying $s_{n1} = ir_{n1}$, as done similarly in (17).

References

[1] J.M. Dudley, F. Dias, M. Erkintalo, G. Genty, Instabilities, breathers and rogue waves in optics, Nat. Photonics 8 (2014) 755.

[2] Nail Akhmediev, Adrian Ankiewicz, J.M. Soto-Crespo, Rogue waves and rational solutions of the nonlinear Schrödinger equation, Phys. Rev. E 80 (2009) 026601.

[3] N. Akhmediev, V.M. Eleonskii, N.E. Kulagin, N-modulation signals in a single-mode optical waveguide under nonlinear conditions, Zh. Eksp. Teor. Fiz. 94 (1988) 159–170, Sov. Phys. JETP 67 (1988) 89–95.

[4] N. Akhmediev, J.M. Soto-Crespo, A. Ankiewicz, Extreme waves that appear from nowhere: on the nature of rogue waves, Phys. Lett. A 373 (2009) 2137–2145.

[5] Adrian Ankiewicz, David J. Kedziora, Nail Akhmediev, Rogue wave triplets, Phys. Lett. A 375 (2011) 2782–2785.

[6] David J. Kedziora, Adrian Ankiewicz, Nail Akhmediev, Circular rogue wave clusters, Phys. Rev. E 84 (2011) 056611.

[7] David J. Kedziora, Adrian Ankiewicz, Nail Akhmediev, Second-order nonlinear Schrödinger equation breather solutions in the degenerate and rogue wave limits, Phys. Rev. E 85 (2012) 066601.

[8] N. Akhmediev, V. Korneev, Modulation instability and periodic solutions of the nonlinear Schrödinger equation, Theor. Math. Phys. 69 (1986) 1089–1093.

[9] N. Akhmediev, V. Eleonskii, N. Kulagin, Exact first-order solutions of the nonlinear Schrödinger equation, Theor. Math. Phys. 72 (1987) 809–818.

[10] D.H. Peregrine, Water waves, nonlinear Schrödinger equations and their solutions, J. Aust. Math. Soc. B 25 (1983) 16.

[11] N.N. Bogoliubov, On the theory of superfluidity, J. Phys. (USSR) 11 (1947) 23; Reprinted in: D. Pine, The Many-Body Problem, Benjamin, New York, 1961, p. 292.

[12] A.L. Fetter, J.D. Walecka, Quantum Theory of Many-Particle Systems, McGraw–Hill, New York, 1971, pp. 317, 493–496.

[13] C.J. Pethick, H. Smith, Bose–Einstein Condensation in Dilute Gases, Cambridge University Press, Cambridge, 2002, pp. 174–177.

[14] T.B. Benjamin, J. Feir, The disintegration of wave trains on deep water, part 1. Theory, J. Fluid Mech. 27 (1967) 417–430.

[15] M. Erkintalo, K. Hammani, B. Kibler, C. Finot, N. Akhmediev, J.M. Dudley, G. Genty, Higher-order modulation instability in nonlinear fiber optics, Phys. Rev. Lett. 107 (2011) 253901.

[16] Nail N. Akhmediev, Nina V. Mitzkevich, Extremely high degree of N-soliton pulse compression in an optical fiber, IEEE J. Quantum Electron. 21 (1991) 849–857.

[17] D.J. Kedziora, A. Ankiewicz, N. Akhmediev, Rogue waves and solitons on a cnoidal background, Eur. Phys. J. Spec. Top. 223 (2014) 43–62.

[18] A. Chowdury, D.J. Kedziora, A. Ankiewicz, N. Akhmediev, Breather-to-soliton conversions described by the quintic equation of the nonlinear Schrödinger hierarchy, Phys. Rev. E 91 (2015) 032928.

[19] B. Kibler, J. Fatome, C. Finot, G. Millot, F. Dias, G. Genty, N. Akhmediev, J. Dudley, The Peregrine soliton in nonlinear fibre optics, Nat. Phys. 6 (10) (2010) 790–795.

[20] B. Frisquet, B. Kibler, G. Millot, Collision of Akhmediev breathers in nonlinear fiber optics, Phys. Rev. X 3 (2013) 041032.

[21] B. Frisquet, A. Chabchoub, J. Fatome, C. Finot, B. Kibler, G. Millot, G. Genty, Two-stage linear–nonlinear shaping of an optical frequency comb as rogue nonlinear-Schrödinger-equation-solution generator, Phys. Rev. A 89 (2014) 023821.

[22] S. Toenger, T. Godin, C. Billet, F. Dias, M. Erkintalo, G. Genty, J.M. Dudley, Emergent rogue wave structures and statistics in spontaneous modulation instability, Sci. Rep. 5 (2015) 10380.

[23] N. Akhmediev, J.M. Soto-Crespo, A. Ankiewicz, How to excite a rogue wave, Phys. Rev. A 80 (2009) 043818.

[24] Siu A. Chin, Omar A. Ashour, Milivoj R. Belić, Anatomy of the Akhmediev breather: cascading instability, first formation time, and Fermi–Pasta–Ulam recurrence, Phys. Rev. E 92 (2015) 063202.

[25] H. Yoshida, Construction of higher order symplectic integrators, Phys. Lett. A 150 (1990) 262–268.